Acta Crystallographica Section F
Structural Biology and Crystallization Communications
ISSN 1744-3091

Structures of new crystal forms of *Mycobacterium tuberculosis* peptidyl-tRNA hydrolase and functionally important plasticity of the molecule

M. Selvaraj, Rais Ahmad, Umesh Varshney and M. Vijayan*

Molecular Biophysics Unit, Indian Institute of Science, Bangalore 560 012, India

Correspondence e-mail: mv@mbu.iisc.ernet.in

Received 6 September 2011
Accepted 4 December 2011

PDB References: *Mt*Pth, form IV, 3tck; form V, 3td2; form V at 50% PEG, 3td6; new form II, 3tcn.

The X-ray structures of new crystal forms of peptidyl-tRNA hydrolase from *M. tuberculosis* reported here and the results of previous X-ray studies of the enzyme from different sources provide a picture of the functionally relevant plasticity of the protein molecule. The new X-ray results confirm the connection deduced previously between the closure of the lid at the peptide-binding site and the opening of the gate that separates the peptide-binding and tRNA-binding sites. The plasticity of the molecule indicated by X-ray structures is in general agreement with that deduced from the available solution NMR results. The correlation between the lid and the gate movements is not, however, observed in the NMR structure.

1. Introduction

A variety of causes result in the premature stalling of translation, leading to the dropping-off of peptidyl-tRNA from the ribosome. Accumulation of peptidyl-tRNA is toxic to the cell and also results in the non-availability of free tRNA for further protein synthesis (Atherly, 1978; Menninger, 1976). This is eventually prevented by the action of the enzyme peptidyl-tRNA hydrolase (Pth), which cleaves the ester bond between tRNA and the peptide, thus releasing tRNA for further use (Cuzin *et al.*, 1967; Kössel & RajBhandary, 1968; Das & Varshney, 2006). In eubacteria Pth is a monomeric enzyme that has been shown to be essential for cell viability and therefore qualifies as a potential drug target. Pth from *Mycobacterium tuberculosis* (*Mt*Pth) is a 191-amino-acid protein coded by the gene Rv1014c. As part of a long-range programme on the structural biology of mycobacterial proteins (Vijayan, 2005; Prabu *et al.*, 2006; Krishna *et al.*, 2007; Roy *et al.*, 2008; Kaushal, Talawar *et al.*, 2008; Chetnani *et al.*, 2010), we cloned, overexpressed, purified and crystallized *Mt*Pth in three crystal forms, which were analyzed by X-ray crystallography (Selvaraj *et al.*, 2006, 2007). In the crystal structure of the *Escherichia coli* enzyme (*Ec*Pth), which has previously been analyzed, the C-terminus of the molecule is bound to the peptide-binding site of the adjacent molecule, which is a cleft between the body of the molecule and a peptide stretch encompassing a loop and a short helix (Schmitt *et al.*, 1997). This stretch closes on the bound C-terminus with a movement similar to that observed in other proteins (Ruzheinikov *et al.*, 2004; Qin *et al.*, 1998; Oliveira *et al.*, 2001). The C-terminal stretch thus mimics the peptide component of the peptidyl-tRNA. In the structure of *Mt*Pth the C-terminal region of the enzyme is disordered and the loop in the peptide-binding region has an open conformation (Selvaraj *et al.*, 2007). Furthermore, the peptide-binding region and tRNA-binding region in *Mt*Pth are not contiguous as the gate separating them has a closed conformation. In the structure of peptide-bound *Ec*Pth, on the other hand, the loop in the peptide-binding region is closed over the bound peptide and the gate separating the two binding regions is open so that peptidyl-tRNA can bind to the enzyme. Thus, together the two structures appeared to describe the structural changes associated with the action of Pth.

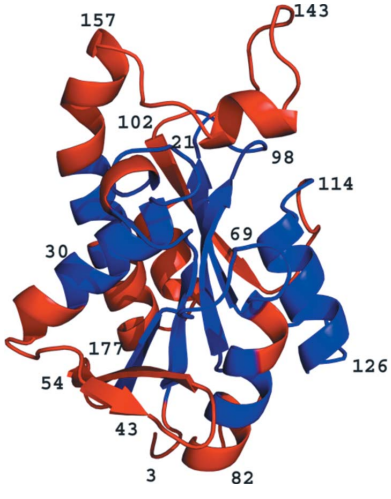

© 2012 International Union of Crystallography
All rights reserved

Table 1
Data-collection and refinement statistics.

Values in parentheses are for the highest resolution shell.

Crystal form (PDB entry)	Form IV (3tck)	Form V (3td2)	Form V at 50% PEG (3td6)	New form II (3tcn)
Space group	$P2_12_12_1$	$P3_221$	$P3_221$	$P2_1$
Unit-cell parameters (Å, °)	a = 36.30, b = 38.81, c = 122.88, $\alpha = \beta = \gamma$ = 90	a = 60.31, b = 60.31, c = 87.67, $\alpha = \beta$ = 90, γ = 120	a = 59.47, b = 59.47, c = 80.42, $\alpha = \beta$ = 90, γ = 120	a = 35.74, b = 73.47, c = 59.95, β = 93.48
Resolution (Å)	2.3 (2.4–2.3)	2.5 (2.6–2.5)	3.2 (3.3–3.2)	2.3 (2.4–2.3)
Temperature (K)	100	100	100	100
V_M (Å^3 Da^{-1})	2.0	2.2	2.0	1.9
Solvent content (%)	38.9	45.8	38.6	35.8
Unique reflections	7780 (1058)	6725 (963)	2900 (404)	13866 (2016)
No. of measured reflections	48028 (6319)	26050 (4010)	11293 (1609)	55589 (8022)
Multiplicity	6.2 (6.0)	3.9 (4.2)	3.9 (4.0)	4.0 (4.0)
Completeness (%)	95.8 (89.4)	99.7 (99.6)	98.9 (100.0)	100.00 (100.00)
Mean $I/\sigma(I)$	11.4 (5.3)	13.3 (2.4)	9.9 (4.3)	10.9 (4.0)
R_{merge}†	15.8 (23.5)	8.1 (47.9)	15.5 (25.7)	13.0 (30.3)
R factor (%)	22.4	23.6	23.1	18.0
R_{free} (%)	26.9	25.5	26.9	22.8
R.m.s. deviation from ideal				
Bond lengths (Å)	0.008	0.009	0.013	0.007
Bond angles (°)	1.8	1.5	1.5	1.5
Ramachandran plot statistics (chain A, B)‡				
Most favoured regions (%)	90.8	90.8	83.9	95.3, 92.8
Favoured regions (%)	5.2	9.2	16.1	3.4, 7.2
Generously allowed regions (%)	2.6	0.0	0.0	0.7, 0.7
Disallowed regions (%)	1.3	0.0	0.0	0.7, 0.0
Residues built in the protein	1–189	1–187	1–184	Chain A, 1–182; chain B, 2–189
No. of molecules in asymmetric unit	1	1	1	2
No. of water molecules	262	72	18	341

† $R_{merge} = \sum_{hkl}\sum_i |I_i(hkl) - \langle I(hkl)\rangle| / \sum_{hkl}\sum_i I_i(hkl)$, where $I_i(hkl)$ is the ith observation of reflection hkl and $\langle I(hkl)\rangle$ is the weighted average intensity for all observations i of reflection hkl. ‡ Calculated for nonglycine and nonproline residues using *PROCHECK*.

Soon after the X-ray structure of *Mt*Pth was reported, the solution structure determined by NMR became available (Pulavarti *et al.*, 2009). Not surprisingly, the molecule has the same overall structure in the crystals and in solution. However, there are notable differences between the crystal and the solution structures. Between nine and 12 C-terminal residues are disordered in the crystal structures, while they form an ordered helix in solution. Perhaps more importantly, the gate separating the two binding regions is closed in the crystal structures while it is open in the solution structure. Thus, it appeared that the structure of *Mt*Pth needed to be further investigated. As an effort in this direction, we have now analyzed two new crystal forms of the enzyme using X-ray crystallography. A previously known crystal form grown in the presence of a pentapeptide was also analyzed. In addition, the effect of partial dehydration on the molecule in one of the new forms was explored. In the meantime, crystal structures of the protein from *M. smegmatis* (*Ms*Pth) became available (PDB entries 3p2j and 3kjz; A. Kumar, A. Singh, R. Yadav, M. Sinha, A. Arora, S. Sharma & T. P. Singh, unpublished work). Most recently, the structure of Pth from *Francisella tularensis* (*Ft*Pth) has been reported (Clarke *et al.*, 2011). These new results are used here to critically examine the functionally relevant plasticity of the molecule deduced from the previously reported structures of *Mt*Pth and *Ec*Pth.

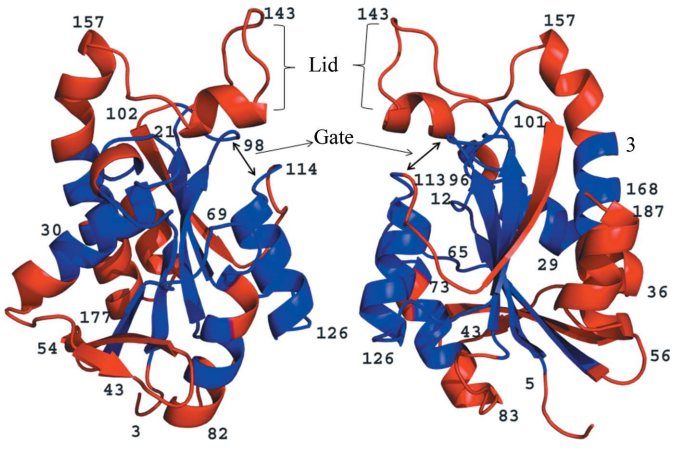

Figure 1
Overall structure of *Mt*Pth viewed from nearly opposite directions. The rigid (blue) and flexible regions (red) of the molecule (see text) are indicated. The locations of the 'lid' and 'gate' are also indicated.

2. Materials and methods

The protein was cloned, expressed and purified following the procedure described previously (Selvaraj *et al.*, 2006). In attempts to grow new crystal forms of the enzyme, crystallization conditions were again explored using Crystal Screen and Crystal Screen 2 from Hampton Research (Jancarik & Kim, 1991). Conditions were also explored around those under which forms I, II and III were obtained using the microbatch-under-oil crystallization method. The same experiments were repeated in crystallization media containing a tenfold molar excess of pentaglycine with respect to the protein concentration. The protein concentration was 10 mg ml^{-1} in all experiments. The experiments yielded two new crystal forms of the enzyme, referred to in the following as forms IV and V. Form IV grew using the same conditions under which forms I and II were obtained (0.1 *M* HEPES pH 7.5, 15% PEG 8000, 5% isopropanol), while form V was obtained using 0.1 *M* HEPES pH 7.5 and 5% dioxane with 25% PEG 8000 as the precipitant. In the presence of the pentapeptide, only form II crystals grew. Form V crystals were partially dehydrated by transferring the crystals from the native conditions to the same conditions with 50% PEG 8000 and leaving them in this solution for a week. X-ray diffraction data were collected at 100 K using a MAR345 image plate mounted on a Rigaku MicroMax-007 rotating-anode X-ray generator with 1° oscillation per frame. The

data were processed using *MOSFLM* and scaled using *SCALA* from the *CCP*4 package (Winn *et al.*, 2011). Molecular replacement was performed using form I *Mt*Pth (PDB entry 2z2i; Selvaraj *et al.*, 2007) as the search model employing *Phaser* (McCoy *et al.*, 2007). Model building was performed using *Coot* (Emsley & Cowtan, 2004). After initial phasing, the model was subjected to rigid-body refinement, positional refinement, torsion-angle refinement and *B*-factor refinement. Refinement was performed using *CNS* v.1.1 after omitting 5% of the reflections for $R_{\rm free}$ calculation (Brünger *et al.*, 1998). Form V crystals were subjected to TLS refinement with the entire protein chain as a single TLS group (Winn *et al.*, 2001). Water O atoms were added at the final stage of refinement where the peak height was greater than 0.8σ in $2F_{\rm o} - F_{\rm c}$ maps and 2.5σ in $F_{\rm o} - F_{\rm c}$ maps.

PROCHECK was used to validate the model (Laskowski *et al.*, 1993). Interatomic distances were calculated using *CONTACT* in *CCP*4 as well as *PyMOL* (DeLano, 2002). Structure superpositions were performed using *ALIGN* (Cohen, 1997). Secondary structures were assigned using *STRIDE* (Frishman & Argos, 1995) and figures were generated using *PyMOL*.

3. Results

3.1. Overall features

The structures of three crystal forms of *Mt*Pth (forms I, II and III) have been reported previously (Selvaraj *et al.*, 2007). Form IV, reported here, grew under the same conditions under which forms I and II were crystallized. The orthorhombic crystals of form IV contained one molecule in the asymmetric unit. Form V was crystallized under slightly different conditions and has one crystallographically independent molecule in the trigonal crystals. Also reported here is the structure of form II crystals, which are monoclinic with two molecules in the asymmetric unit, grown in the presence of pentaglycine. The structures mentioned above were determined to a resolution of 2.3–2.5 Å (Table 1). A partially dehydrated form of the form V crystals could be obtained by soaking the crystals in the crystallization solution with high PEG content. The structure of this partially dehydrated form was also determined, for reasons that will be discussed later. Attempts to partially dehydrate the other crystal forms resulted in unacceptable deterioration of diffraction quality.

As in the previously reported Pth structures and the structure of the homologous chloroplast group II intron splicing factor 2 (CRS2; Ostheimer *et al.*, 2005), the molecules in the crystal forms presented here adopt an α/β-fold with a twisted β-sheet flanked by helices (Fig. 1). In forms I, II and III the last 9–12 residues in the 191-amino-acid polypeptide chain were disordered. In contrast, much of the C-terminal stretch is ordered in the structures reported here. In the molecule in form IV the chain could be traced to 189 residues. Side chains were not clear in parts of this stretch. Therefore, only a poly-Ala model could be built for residues 184–188. The molecule in form V could be traced to 186 residues. In the low-water-content form the chain could only be traced to residue 184. No bound peptide could be located in form II crystals grown in the presence of pentaglycine. However, unlike in the original form II crystals, the polypeptide chain could be traced to 182 and 187 residues in the two molecules in these crystals. Therefore, while only 179–182 residues were defined in all of the crystal structures reported previously, the remaining residues are defined to different extents in those reported here.

3.2. Plasticity

The availability of several crystal structures of the molecule permit an exploration of the plasticity of *Mt*Pth. The published NMR results provide additional information. Analysis using the *Error-inclusive Structure Comparison and Evaluation Tool* (*ESCET*), involving weighted difference distance matrices, facilitates a rough-and-ready delineation of the relative rigid and flexible regions of the molecule (Schneider, 2002). The results obtained when the appropriate parameter is chosen so as to divide the molecule nearly equally into rigid and flexible regions are illustrated in Fig. 1. They are in reasonable agreement with the NMR results (Pulavarti *et al.*, 2009). As expected,

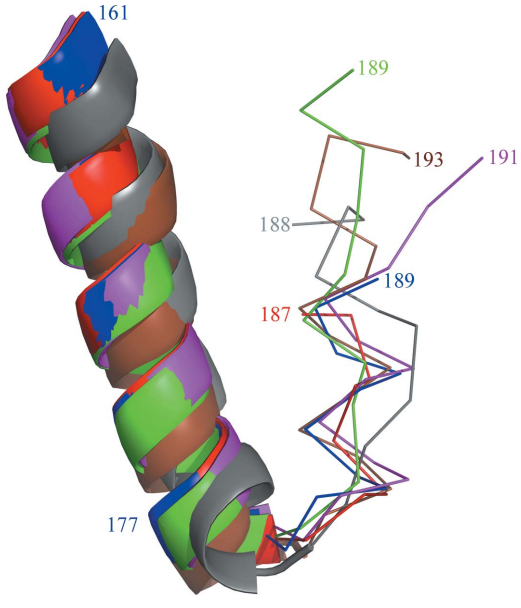

Figure 2
The C-terminal stretch as observed in *Mt*Pth form II molecule *B* (blue), *Mt*Pth form IV (green), *Mt*Pth form V (red), *Ec*Pth (brown), *Ms*Pth (magenta) and *Ft*Pth (grey).

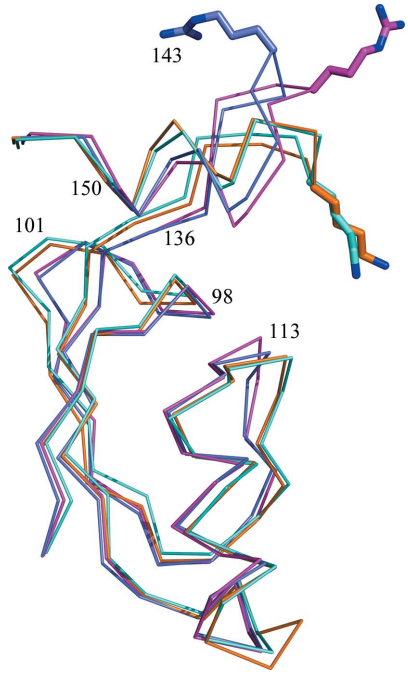

Figure 3
Conformation of the lid in *Mt*Pth form I (blue), *Ms*Pth (magenta), *Ec*Pth (brown) and *Ft*Pth (cyan).

Table 2
Lid and gate distances (see text) in the relevant crystal structures.

Pth crystal structure (PDB entry)	Distance (Å)	
	Lid (Arg143 CA···Val92 CA)†	Gate (Asp98 CA···Gly113 CA)‡
*Mt*Pth form I (2z2i)	29.4	6.4
*Mt*Pth form II, molecule *A* (2z2j)	29.4	6.2
*Mt*Pth form II, molecule *B* (2z2j)	29.3	6.1
*Mt*Pth form III (2z2k)	28.0	6.3
*Mt*Pth form V (3td2)	29.3	6.2
*Mt*Pth new form II, molecule *A* (3tcn)	29.2	6.3
*Mt*Pth new form II, molecule *B* (3tcn)	29.1	6.2
*Ms*Pth form I (3p2j)	28.7	7.1
*Ms*Pth form II (3kjz)	28.6	7.4
*Ec*Pth (2pth)	23.6	9.5
*Ft*Pth (3nea)	23.4	10.0

† Lys142/143 CA···Val90/92 CA in *Ec*Pth and *Ft*Pth. ‡ Asp96 CA···Gly111 CA in *Ec*Pth.

the core of the molecule is substantially rigid, while the periphery is by and large flexible. The division in terms of secondary-structural features is less clear. Helices or parts thereof, strands and loops are found in rigid as well as flexible regions. The C-terminal stretch involving the last 12 residues appears to constitute the most variable region of the molecule. The region is ill-defined and presumably disordered in some crystal structures of *Mt*Pth. Substantial variability between structures is exhibited by this stretch in the crystal structures in which it is ordered (Fig. 2). The solution structure has a single helical conformation for the C-terminal stretch, but with considerable flexibility. The lid region, involving a helix and a loop (Gly136–Val150), which has been suggested to close on the bound peptide, is in the flexible region. The same is true for part of the loop which contains one of the gate residues (Gly113). The other gate residue (Asp98) is in a relatively rigid region. The same trend is seen in the solution structure. Yet another flexible stretch is the 50–60 loop, which is flanked by one end of the highly flexible C-terminal stretch and the flexible N-terminal residues. In fact, this loop forms part of a contiguous flexible region on one side of the molecule.

3.3. The lid and the gate

The movement of the lid region (Gly136–Val150) and the gate (Asp98–Gly113) between the peptide-binding and tRNA-binding sites is of particular interest. A careful examination indicated that the lid movement can be described in terms of the distance between the C^{α} position of Val92, which is an invariant residue in a rigid region of the core of the molecule, and the C^{α} position of Arg143 (or Lys142 in *Ec*Pth and Lys143 in *Ft*Pth) at the tip of the lid. Among the enzymes of known structure from different species, the former residue is Val90 in *Ec*Pth, Val92 in *Ms*Pth and Val92 in *Ft*Pth. The movement of the gate can obviously be discussed in terms of the distance between the C^{α} positions of the two gate residues Asp98 and Gly113. These residues are also invariant among Pths of known structure.

The lid and the gate residues are on the surface of the molecule and hence it is important to ascertain the effect of crystal contacts, if any, on their conformations. Detailed calculations showed that the lid in form IV is involved in crystal contacts. A conformation of the lid similar to that in other *Mt*Pth crystal structures would lead to serious steric clashes in form IV. Therefore, the lid adopts a somewhat closed conformation, presumably to avoid these clashes. Hence, among the crystal structures of *Mt*Pth, form IV was removed from the discussion of the movement of the lid and the gate residues.

The conformation of the lid in representative crystal structures of Pth is illustrated in Fig. 3. The distances that indicate the state of the lid and the gate in the relevant crystal structures are listed in Table 2. The two distances are correlated, as indeed are the corresponding conformations (Fig. 4*a*). In the structures of the two mycobacterial Pths with no peptide in the binding site the lid has an open conformation and the gate is closed. The reverse is true in the crystal structures of *Ec*Pth and *Ft*Pth, in both of which the peptide-binding site is occupied by the C-terminal residues of a neighbouring molecule. Thus, the model of the internal movements of Pth associated with enzyme action proposed previously on the basis of the crystal structures of *Ec*Pth and *Mt*Pth (Selvaraj *et al.*, 2007) appears to have been confirmed by the crystal structures which subsequently became available.

As indicated previously, the solution structure of *Mt*Pth presents a somewhat different picture. As expected, the lid and the gate distances exhibit substantial variability. The lid distances in the 40 models vary between 25.3 and 31.7 Å, with an average value of 28.5 Å, which is comparable to those in the crystal structures of mycobacterial Pths. The gate distance varies between 8.6 and 17.7 Å, with an average value of 12.6 Å, which is even greater than those in the crystal structures of *Ec*Pth and *Ft*Pth. Furthermore, there is only a very weak correlation, if any, between the two distances (Fig. 4*b*).

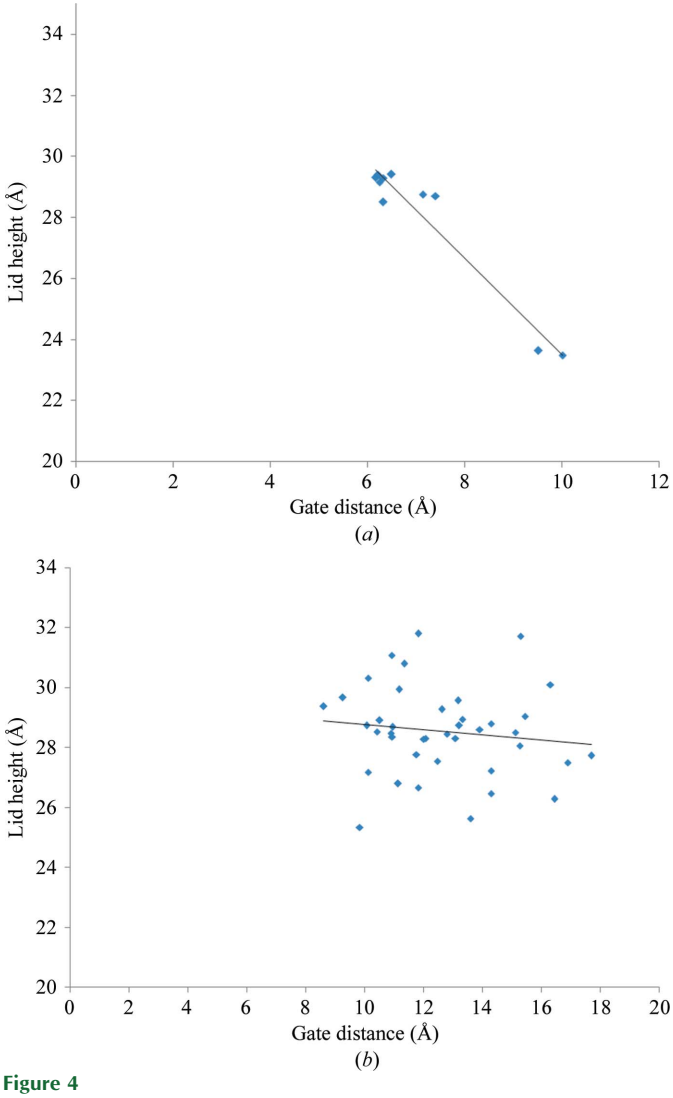

Figure 4
Correlation between gate and lid distances in (*a*) available crystal structures and (*b*) NMR structures.

Previous studies in this laboratory indicated that partial dehydration of protein crystals could elicit movements similar to those that occur during protein action (Kodandapani *et al.*, 1990; RadhaKishan *et al.*, 1995; Vijayalakshmi *et al.*, 2008; Kaushal, Sankaranarayanan *et al.*, 2008). This was the rationale for attempting to partially dehydrate *Mt*Pth crystals. Attempts only succeeded in the case of form V. Form V crystals diffracted reasonably well even when they were soaked in a solution containing 50% PEG to reduce the level of hydration. In the crystal structure of low solvent-content form V, the gate opens to a distance of 8.5 Å, compared with a distance of 6.2 Å in the native form V crystals. This lends additional support to the earlier suggestion that opening of the gate is associated with enzyme action.

4. Discussion

The structural studies considered here appear to establish a relationship between the flexibility of certain regions of the molecule and their biological role. The most flexible region of the molecule is the C-terminal stretch. It is disordered to different extents in many crystal structures. Its conformation differs substantially among those structures in which the stretch is reasonably well defined. It is helical, but is flexible in solution. This flexibility appears to be related to its biological function, which has been reported to be interaction with the TψC loop of tRNA (Fromant *et al.*, 1999). This flexibility is perhaps necessary for the peptide stretch to wrap around the loop.

The peptide stretch that makes up the lid and the loop that carries one of the gate residues also exhibit considerable flexibility, which is obviously required for their biological function. The crystal structures of *Mt*Pth (several forms), *Ms*Pth (two forms), *Ec*Pth and *Ft*Pth appear to provide a clear picture of the correlation between the two movements. The free enzyme has an open lid and a closed gate. When the peptide component of the substrate binds to the peptide-binding region the lid closes on it, with a consequent opening of the gate between the peptide-binding and tRNA-binding regions, facilitating the binding of peptidyl-tRNA to the enzyme prior to hydrolysis. The opening of the gate in response to a reduction in the level of hydration can be taken as an indication of its relevance to function. What is intriguing is that the correlation between the loop movement and the gate movement, which is so unambiguously indicated by the crystal structures, is not clearly seen in the NMR results. This discrepancy merits further investigation.

The X-ray intensity data were collected at the X-ray Facility for Structural Biology at the Molecular Biophysics Unit, supported by the Department of Science and Technology, Government of India. Computations for structure analysis and molecular simulations were performed at the Interactive Graphics Facility supported by the Department of Biotechnology (DBT). The present work forms part of a DBT-sponsored project. MS was a CSIR research fellow and MV is a DAE Homi Bhabha Professor.

References

Atherly, A. G. (1978). *Nature (London)*, **275**, 769.
Brünger, A. T., Adams, P. D., Clore, G. M., DeLano, W. L., Gros, P., Grosse-Kunstleve, R. W., Jiang, J.-S., Kuszewski, J., Nilges, M., Pannu, N. S., Read, R. J., Rice, L. M., Simonson, T. & Warren, G. L. (1998). *Acta Cryst.* D**54**, 905–921.
Chetnani, B., Kumar, P., Surolia, A. & Vijayan, M. (2010). *J. Mol. Biol.* **400**, 171–185.
Clarke, T. E., Romanov, V., Lam, R., Gothe, S. A., Peddi, S. R., Razumova, E. B., Lipman, R. S. A., Branstrom, A. A. & Chirgadze, N. Y. (2011). *Acta Cryst.* F**67**, 446–449.
Cohen, G. H. (1997). *J. Appl. Cryst.* **30**, 1160–1161.
Cuzin, F., Kretchmer, N., Greenberg, R. E., Hurwitz, R. & Chapeville, F. (1967). *Proc. Natl Acad. Sci. USA*, **58**, 2079–2086.
Das, G. & Varshney, U. (2006). *Microbiology*, **152**, 2191–2195.
DeLano, W. L. (2002). http://www.pymol.org.
Emsley, P. & Cowtan, K. (2004). *Acta Cryst.* D**60**, 2126–2132.
Frishman, D. & Argos, P. (1995). *Proteins*, **23**, 566–579.
Fromant, M., Plateau, P., Schmitt, E., Mechulam, Y. & Blanquet, S. (1999). *Biochemistry*, **38**, 4982–4987.
Jancarik, J. & Kim, S.-H. (1991). *J. Appl. Cryst.* **24**, 409–411.
Kaushal, P. S., Sankaranarayanan, R. & Vijayan, M. (2008). *Acta Cryst.* F**64**, 463–469.
Kaushal, P. S., Talawar, R. K., Krishna, P. D. V., Varshney, U. & Vijayan, M. (2008). *Acta Cryst.* D**64**, 551–560.
Kishan, R. V. R., Chandra, N. R., Sudarsanakumar, C., Suguna, K. & Vijayan, M. (1995). *Acta Cryst.* D**51**, 703–710.
Kodandapani, R., Suresh, C. G. & Vijayan, M. (1990). *J. Biol. Chem.* **265**, 16126–16131.
Kössel, H. & RajBhandary, U. L. (1968). *J. Mol. Biol.* **273**, 389–401.
Krishna, R., Prabu, J. R., Manjunath, G. P., Datta, S., Chandra, N. R., Muniyappa, K. & Vijayan, M. (2007). *J. Mol. Biol.* **367**, 1130–1144.
Laskowski, R. A., Moss, D. S. & Thornton, J. M. (1993). *J. Mol. Biol.* **231**, 1049–1067.
McCoy, A. J., Grosse-Kunstleve, R. W., Adams, P. D., Winn, M. D., Storoni, L. C. & Read, R. J. (2007). *J. Appl. Cryst.* **40**, 658–674.
Menninger, J. R. (1976). *J. Biol. Chem.* **251**, 3392–3398.
Oliveira, K. M., Valente-Mesquita, V. L., Botelho, M. M., Sawyer, L., Ferreira, S. T. & Polikarpov, I. (2001). *Eur. J. Biochem.* **268**, 477–483.
Ostheimer, G. J., Hadjivassiliou, H., Kloer, D. P., Barkan, A. & Matthews, B. W. (2005). *J. Mol. Biol.* **354**, 51–68.
Prabu, J. R. *et al.* (2006). *Acta Cryst.* F**62**, 731–734.
Pulavarti, S. V., Jain, A., Pathak, P. P., Mahmood, A. & Arora, A. (2009). *J. Mol. Biol.* **378**, 165–177.
Qin, B. Y., Bewley, M. C., Creamer, L. K., Baker, H. M., Baker, E. N. & Jameson, G. B. (1998). *Biochemistry*, **37**, 14014–14023.
Roy, S., Saraswathi, R., Gupta, S., Sekar, K., Chatterji, D. & Vijayan, M. (2008). *J. Mol. Biol.* **370**, 752–767.
Ruzheinikov, S. N., Das, S. K., Sedelnikova, S. E., Baker, P. J., Artymiuk, P. J., García-Lara, J., Foster, S. J. & Rice, D. W. (2004). *J. Mol. Biol.* **339**, 265–278.
Schmitt, E., Mechulam, Y., Fromant, M., Plateau, P. & Blanquet, S. (1997). *EMBO J.* **16**, 4760–4769.
Schneider, T. R. (2002). *Acta Cryst.* D**58**, 195–208.
Selvaraj, M., Roy, S., Singh, N. S., Sangeetha, R., Varshney, U. & Vijayan, M. (2007). *J. Mol. Biol.* **372**, 186–193.
Selvaraj, M., Singh, N. S., Roy, S., Sangeetha, R., Varshney, U. & Vijayan, M. (2006). *Acta Cryst.* F**62**, 913–915.
Vijayalakshmi, L., Krishna, R., Sankaranarayanan, R. & Vijayan, M. (2008). *Proteins*, **71**, 241–249.
Vijayan, M. (2005). *Tuberculosis (Edinb.)*, **85**, 357–366.
Winn, M. D. *et al.* (2011). *Acta Cryst.* D**67**, 235–242.
Winn, M. D., Isupov, M. N. & Murshudov, G. N. (2001). *Acta Cryst.* D**57**, 122–133.